A Prediction Model for Functional Outcomes in Spinal Cord Disorder Patients Using Gaussian Process Regression

Sunghoon Ivan Lee, *Student Member, IEEE*, Bobak Mortazavi, *Student Member, IEEE*, Haydn A. Hoffman, Derek S. Lu, Charles Li, Brian H. Paak, Jordan H. Garst, Mehrdad Razaghy, Marie Espinal, Eunjeong Park, *Member, IEEE*, Daniel C. Lu, and Majid Sarrafzadeh, *Fellow, IEEE*

***Abstract*—Predicting the functional outcomes of spinal cord disorder patients after medical treatments, such as a surgical operation, has always been of great interest. Accurate posttreatment prediction is especially beneficial for clinicians, patients, care givers, and therapists. This paper introduces a prediction method for postoperative functional outcomes by a novel use of Gaussian process regression. The proposed method specifically considers the restricted value range of the target variables by modeling the Gaussian process based on a truncated Normal distribution, which significantly improves the prediction results. The prediction has been made in assistance with target tracking examinations using a highly portable and inexpensive handgrip device, which greatly contributes to the prediction performance. The proposed method has been validated through a dataset collected from a clinical cohort pilot involving 15 patients with cervical spinal cord disorder. The results show that the proposed method can accurately predict postoperative functional outcomes, Oswestry disability index and target tracking scores, based on the patient's preoperative information with a mean absolute error of 0.079 and 0.014 (out of 1.0), respectively.**

***Index Terms*—Functional outcomes, gaussian process regression (GPR), handgrip, prediction, spinal cord disorder, target tracking, truncated normal distribution.**

I. Introduction

THERE are approximately 400 000 patients suffering from spinal cord disorder in the United States, with nearly 15 000 new patients each year [1], [2]. The chronic or traumatic degeneration in the spine results in reduction of the spinal canal diameter and compresses the spinal cord, which impairs the transmission of electrical signals and results in partial or complete loss of sensory and/or motor function [1]. The physiological symptoms of spinal cord disorder that are associated with hand movements include the loss of hand dexterity, numbness, stiffness, weakness, fatigue, and termor. As a consequence, patients with spinal disorder often have problems coordinating fine movements using hand muscles, which restricts various daily activities such as eating, bathing, or lifting small objects [3].

There exist various methods that quantify physical conditions and/or the level of motor deficits of spinal disorder patients such as radiological imaging (e.g., X-ray, MRI, and CT) [4], clinicians observations (e.g., finger-to-nose or heel-to-shin examinations) [5], and patient-reported functional outcomes [6]–[8]. Among these techniques, patients' self-ratings of perceived level of motor function and quality of life, such as the Oswestry disability index (ODI) [6] and short form 36 (SF-36) [7], have been widely used as primary measures for clinical effectiveness [8] since the fundamental objective of medical treatment is to improve the well being of patients [9].

Predicting the patient-reported functional level after medical treatments (e.g., surgical operations, rehabilitation, or medication) has always been of great interest [10]-[12]. Regression based on various demographic and clinical variables has been the most commonly used prediction platform since patient-reported outcomes are often close to real values. Most existing works employ regression models that assume a predefined relationship (i.e., often linear) between the predictors and the outcome. Although these methods can be implemented easily and provide clear interpretability, they have two major shortcomings. First, the assumption of a predefined relationship (e.g., polynomial or exponential) may not necessarily be true because one form of measure may be more sensitive at a certain range of physical conditions than others. Second, these types of regression methods focus on fitting the data points to minimize the prediction error, and as a result, they produce a single best value rather than providing a probabilistic prediction (i.e., predictive distribution); predictive distribution is especially important since it provides a comprehensive summary about the prediction. For instance, the predictive distribution can be utilized to more accurately model the distribution of target variables with restricted value range, as will be discussed in the remaining of this paper.

This paper introduces a prediction method for postoperative functional outcomes using Gaussian process regression (GPR), which specifically addresses the aforementioned shortcomings

Manuscript received January 22, 2014; revised September 19, 2014; accepted November 6, 2014. Date of publication November 20, 2014; date of current version December 31, 2015.

S. I. Lee, B. Mortazavi, E. Park, and M. Sarrafzadeh are with the Computer Science Department and the Wireless Health Institute, University of California Los Angeles, Los Angeles CA 90095 USA (e-mail: silee@cs.ucla.edu; bobakm@cs.ucla.edu; ejpark@cs.ucla.edu; majid@cs.ucla.edu).

H. A. Hoffman, D. S. Lu, C. Li, B. H. Paak, J. H. Garst, M. Razaghy, and M. Espinal are with the Department of Neurosurgery, University of California Los Angeles, Los Angeles, CA 90095 USA (e-mail: hhoffman@mednet.ucla.edu; dslu@mednet.ucla.edu; chli@mednet.ucla.edu; bhpaak@gmail.com; jordanhaywardgarst@gmail.com; mehrdad.mro@gmail.com; marie.espinal1@gmail.com).

D. C. Lu is with the Department of Neurosurgery and the Department of Orthopedic Surgery, University of California Los Angeles, Los Angeles, CA 90095 USA (e-mail: dclu@mednet.ucla.edu).

Color versions of one or more of the figures in this paper are available online at http://ieeexplore.ieee.org.

Digital Object Identifier 10.1109/JBHI.2014.2372777

of the existing prediction methods. Additionally, the proposed method introduces a novel modeling of GPR based on a truncated Normal distribution, which is designed to consider the restricted value range of the target variable. The proposed prediction method is performed in assistance with a simple target tracking examination using a lightweight and inexpensive handgrip device, which contribute significantly to prediction performance. Target tracking based on the grip strength is known to effectively quantify the motor condition of patients with hand movement deficits such as Parkinson's disease [13], stroke [14], chronic inflammatory demyelinating polyneuropathy (CIDP) [15], and spinal cord disorder [16]. Note that the proposed method is not only limited to the spinal cord disorder population but can also be applied to other ailments as this paper provides the design and parametrization details of applying GPR for motor function prediction.

II. Related Works

Predicting perceived motor function and health-related quality of life in spinal disorder patients has been of great interest [10]–[12]. Authors in [10] used multivariate linear regression to find correlation to the health-related instrument: Sickness Impact Profile (SIP68). Similar studies have been performed in [11] and [12], where the authors have used hierarchical multiple linear regression and step-wise linear regression as the prediction models, respectively. Both studies compared the life satisfaction to various demographic and clinical parameters including gender, age, and number of rehospitalizations.

Prediction of perceived motor function is also an active research topic in other ailments carrying motor deficits. For example, Veerbeek *et al.* [17] reviewed 48 articles on prediction of functional outcomes in patients with stroke. All studies reviewed by Veerbeek *et al.* [17] employed either linear or logistic regression for prediction. Similarly, Soh *et al.* [18] reviewed 29 articles that predict health-related quality of life in Parkinson's disease. This paper reports that multivariate regression was the most frequently used prediction platform followed by step-wise linear regression and hierarchical multivariate linear regression.

Although the aforementioned works examine various variables for predicting self-reported functional outcomes, these prediction models suffer from the shortcomings discussed in the previous section. GPR has recently received much attention as a solution to these problems in various fields including biomedical engineering [19] and clinical research [20]. To the best of the authors' knowledge, this paper is the first attempt to apply GPR in predicting postoperative functional outcomes in patients with movement disorders.

III. Materials

A. Cohort Clinical Trial

This paper validates the prediction methods using a dataset collected from a 24-month-long cohort trial. A total of 34 cervical spinal cord disorder patients with hand movement deficits were recruited through the UCLA Spine Center. Seven of these patients decided to drop out of the study, and nine patients were new patients whose three months postoperative data has not yet been collected. Data collected from three patients were corrupted and removed from the study due to either mistakes during the data collection process or malfunction of the system itself. As a consequence, this study is validated through a dataset collected from 15 patients (mean age of 62.3 and a std. dev. of 13.1). All patients have received a surgical decompression operation that alleviates the nerve pressure on the spine, performed by a single neurosurgeon. The examination procedure was approved by the UCLA institutional review board, and all patients provided consent to participate in the study.

B. Measure of Self-Reported Motor Function

There exist various forms of self-reported functional outcomes. The ODI has been used as one of the primary condition-specific assessment tools for general spinal cord disorder patients [6] as well as patients with upper limb deficits [21]. The ODI is a survey consisting of ten questionnaires regarding the level of pain in the affected area and the degree of disabilities in everyday activities such as sleeping, self-care, sex life, social life, and traveling [21]. Each question has five or six answer choices, and patients must select the one that best describes the effect of pain in performing these activities. The accumulated score is linearly scaled to [0, 1] based on the number of available choices, where zero indicates completely disabled conditions in performing the specified activity, and one indicates completely healthy condition.

C. Demographic and Clinical Variables

The objective of this paper is to introduce a prediction method for postoperative functional outcomes based on a patient's preoperative information. Various clinical and demographic variables are considered in this study based on previous findings [22]: age, narrowest diameter of the spinal canal before surgery, and months after injury. The narrowest diameter of the spinal canal is measured using the conventional X-ray imaging. The number of months after injury is reported by patients.

D. Measure of Objective Fine-Motor Function

The prediction of postoperative condition is performed in assistance with a especially designed handgrip device and target tracking tests, which have been validated for its clinical effectiveness in quantifying hand motor function [16]. The handgrip device is illustrated in Fig. 1(a). All tracking tests are normalized to the patient's maximum voluntary contraction, which represents the maximum grip strength that a patient can voluntarily exert, in order to accommodate patients with different grip strengths.

The test is performed on two different target functions as shown in Fig. 1(b): sinusoidal and step functions. The sinusoidal function is known to examine the motor-learning capability for fine muscle control, and the step function is known to investigate a patient's ability to predict and execute relatively rapid hand movements [23]. As the test begins, the target within the screen

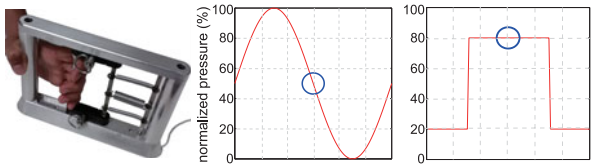

(a) (b)

Fig. 1. (a) Handgrip device using in this study to quantify the hand motor capacity of cervical spinal disorder patients. (b) Two target functions used in this study: sinusoidal (left) and step (right).

moves toward the left at a constant speed. The blue circle is always located in the middle of the horizontal axis, but its vertical position varies according to the applied grip strength. The length of the test is 45 s. The objective of the test is to minimize the error between the target and the patient's response. Mean absolute error (MAE) is the most frequently used motor measure [23], which computes mean absolute difference between the target and the patient's response over the period of the test. This paper follows the *general system performance theory* that all dimensions of human performance are in a form for which a higher numerical value represents superior performance [24]. Therefore, the Mean absolute accuracy (MAA), which is computed as (1 − MAE), is used as the primary metric for quantifying motor level. Patients were asked to repeat the tracking tests three times, and the average MAA of the three tests was used as the final measure.

E. Longitudinal Study

Patients were asked to visit the clinic at least once prior to the operation. Then, patients were scheduled to have a follow-up visit at least three months after the surgery, since a three-month period is a clinically meaningful time for recovery [8]. Both self-reported functional outcomes and the target tracking results were collected at each clinical visit.

IV. Prediction Methodology

This section discusses the prediction method in detail, which estimates the postoperative conditions of patients given their preoperative information. The independent variables (or predictors) include preoperative ODI scores (denoted as ρ), preoperative MAA scores of sinusoidal (denoted as α) and step tracks (denoted as β), age (denoted as g), narrowest diameter of the spinal canal before surgery (denoted as r), and months after injury (denoted as h). Two dependent (or target) variables are considered in this study: postoperative ODI score (denoted as ρ') and equally weighted average of postoperative MAA scores of sinusoidal and step tracks (i.e., $\frac{1}{2}(\alpha' + \beta')$). Some of the important notations used in the rest of this paper are listed in Table I.

A. Background

Prediction problems often involve a finite set of independent variables $\boldsymbol{X}$ (i.e., preoperative data of patients) and the associated noisy observation of a dependent variable $\boldsymbol{y}$ (i.e., postoperative data of patients). $\boldsymbol{X}$ is an $n \times d$ matrix, where n represents the number of data points (i.e., the number of patients in this context) and d represents the size of variable dimension. $\boldsymbol{X}$ can be written as $\boldsymbol{X} = \{\boldsymbol{x}_i | i = 1, ..., n\}$ where $\boldsymbol{x}_i$ is a vector of dimension d and $\boldsymbol{y}$ is the target (or observation) vector of size n. The relationship between the input vector and the output variable can be written as

$$y_i = f(\boldsymbol{x}_i) + \varepsilon \tag{1}$$

where $f_i = f(\boldsymbol{x}_i)$ is the latent (hidden) variable that is a function of the data belonging to the patient i, and ε represents the noise added to the observed variables. Then, the prediction problem can be stated as the following: given a training dataset $D = \{\boldsymbol{X}, \boldsymbol{y}\}$, find the best estimate of the dependent variable y_* of a new testing set.

Since the dependent variables are close to real values, the prediction problem can be formalized in a regression setting. GPR is a nonparametric regression model that constructs a relationship between $\boldsymbol{X}$ and $\boldsymbol{y}$ based on the geometric positions of $\boldsymbol{x}_i \forall i$ within the feature space. $\boldsymbol{y}$ is considered as a collection of samples from an n-variate Gaussian distribution, and it allows GPR to provide not only the expected value of $f_* = f(\boldsymbol{x}_*)$, but also the variance of f_*.

TABLE I
Summary of Important Notations Used in this Paper

Symbol	Description
n	Number of data points (patients)
d	Size of feature dimension
$\boldsymbol{X}$	$n \times d$ training design matrix
$\boldsymbol{y}$	$n \times 1$ training observation vector
$\boldsymbol{x}_*$	$1 \times d$ testing vector
y_*	prediction variable
ρ, ρ'	ODI score at pre-, postsurgery
α, α'	Sinusoidal MAA at pre-, postsurgery
β, β'	Step MAA at pre-, postsurgery
g	Age
r	Narrowest diameter of spinal canal
h	Months after injury

B. GPR

This section briefly reviews the fundamental concepts of GPR; the reader is referred to [25] for an in-depth review. The formal definition of a *Gaussian process* is a collection of a finite number of random variables, which has a joint Gaussian distribution [25], and it can be completely defined by its mean function $E[f(\boldsymbol{x})]$ and a covariance function (also known as kernel function) $k(\boldsymbol{x}, \boldsymbol{x'})$: $f(\boldsymbol{x}) \sim GP\left(E[f(\boldsymbol{x})], k(\boldsymbol{x}, \boldsymbol{x'})\right)$. This study employs the *squared exponential* covariance function, which is defined as

$$k(\boldsymbol{x}, \boldsymbol{x'}) = \sigma_f^2 \exp\left(-\frac{1}{2}(\boldsymbol{x} - \boldsymbol{x'})^T M (\boldsymbol{x} - \boldsymbol{x'})\right)$$

where σ_f^2 represents the signal variance and $M = \text{diag}(\ell)^{-2}$ where $\ell = \{\ell_k | k = 1, ..., d\}$. ℓ_k represent *characteristic length-scale* for each input dimension, and M forms a $d \times d$ matrix

with its diagonal consisting of $1/\ell_k^2$ and zero elsewhere. These parameters define the relationship between each of the independent variables and the target variable; it allows different relationships for different independent variables.

Given the training dataset $D = \{\boldsymbol{X}, \boldsymbol{y}\}$ and the testing input vector $\boldsymbol{x_*}$, the joint distribution of the observed dependent variable $\mathbf{y}$ and the latent variable f_* can be written in a matrix form as

$$\begin{bmatrix} \boldsymbol{y} \\ f_* \end{bmatrix} \sim N\left(\begin{bmatrix} \boldsymbol{\mu} \\ \mu_* \end{bmatrix}, \begin{bmatrix} K(\boldsymbol{X}, \boldsymbol{X}) + \sigma_n^2 \boldsymbol{I} & K(\boldsymbol{X}, \boldsymbol{x}_*) \\ K(\boldsymbol{x}_*, \boldsymbol{X}) & K(\boldsymbol{x}_*, \boldsymbol{x}_*) \end{bmatrix} \right)$$

where $K(\boldsymbol{X}, \boldsymbol{x}_*)$ is a $n \times 1$ vector that represents covariance between each data point in $\mathbf{X}$ and $\mathbf{x}_*$. $K(\boldsymbol{X}, \mathbf{X})$, $K(\mathbf{x}_*, \mathbf{X})$, and $K(\mathbf{x}_*, \mathbf{x}_*)$ are also defined in a similar manner. $\boldsymbol{I}$ is an identity matrix and σ_n^2 is the variance in the observed noise ε in (1) assuming that ε is an independently and identically distributed Gaussian distribution: $\varepsilon \sim N(0, \sigma_n^2)$. A collection of free parameters $\boldsymbol{\theta} = \{\ell, \sigma_{\mathbf{f}}^2, \sigma_{\mathbf{n}}^2\}$ is named *hyperparameters*. A method for determining the hyperparameters from training data will be discussed in Section IV-C.

The conditional distribution of the latent variable f_* is also a Gaussian: $\overline{f_*} = f_* | \boldsymbol{X}, \boldsymbol{y}, \boldsymbol{x}_* \sim N(\mu_{\overline{f}_*}, \sigma^2_{\overline{f}_*})$. Note that $\mu_{\overline{f}_*}$ represents the expected value of the latent variable, and the variance $\sigma^2_{\overline{f}_*}$ can be used to compute the confidence range about the prediction. These two values can be computed based on the *multivariate Gaussian theorem* as

$$\begin{aligned} \mu_{\overline{f}_*} &= E(f_* | \boldsymbol{X}, \boldsymbol{y}, \boldsymbol{x}_*) \\ &= \mu_* + K(\boldsymbol{x}_*, \boldsymbol{X})\big[K(\boldsymbol{X}, \boldsymbol{X}) + \sigma_n^2 I\big]^{-1}(\mathbf{y} - \mu) \\ \sigma^2_{\overline{f}_*} &= K(\boldsymbol{x}_*, \boldsymbol{x}_*) \\ &\quad - K(\boldsymbol{x}_*, \boldsymbol{X})\big[K(\boldsymbol{X}, \boldsymbol{X}) + \sigma_n^2 I\big]^{-1} K(\boldsymbol{X}, \boldsymbol{x}_*). \end{aligned} \tag{2}$$

Then, the expected value and the variance of the prediction variable y_* can be easily computed as $\mu_{\overline{y}_*} = \mu_{\overline{f}_*}$ and $\sigma^2_{\overline{y}_*} = \sigma^2_{\overline{f}_*} + \sigma_n^2$, respectively.

C. Hyperparameters

There exist various methods to find the values of hyperparameters $\boldsymbol{\theta} = \{\ell, \sigma_{\mathbf{f}}, \sigma_{\mathbf{n}}\}$ such as maximizing *a posteriori* estimates or the Markov chain Monte Carlo method [25]. This paper employs a method that integrates over the hyperparameters to produce the conditional distribution of the latent variable $\overline{f_*}$, which is known to be more robust to relatively small sized training sets. This method approximates the continuous integration over the hyperparameters using a discrete summation, and the reader is directed to [26] for more detail information.

D. Truncated-GPR

The limitation of applying GPR for predicting postoperative ODI and MAA scores is raised by the fact that the prediction variable $\overline{y}_*$ assumes a Gaussian distribution, which in theory has a distribution over an infinite range. However, the values of ODI and MAA scores are restricted to be within $[0, 1]$, and GPR clearly does not account for this restricted range.

In this study, a novel mapping procedure is proposed to allow predictions to be made in the restricted range of the prediction variables, which is built on the fundamentals of GPR. This mapping procedure can be divided into two major steps: 1) evaluating the latent variable f_* with prior knowledge that the training observation variable $\boldsymbol{y}$ has a range of $[0, 1]$, and 2) the mapping from the output latent variable f_* to y'_*. For simplicity, the following derivation of $p(y'_* | \boldsymbol{X}, \boldsymbol{y}, \boldsymbol{x}_*)$ assumes noise-free observations, i.e., $\varepsilon = 0$ and $\boldsymbol{y} = f(\boldsymbol{X})$ as opposed to (1). The addition of noise variance will be discussed afterwards.

The prediction variable y'_* is assumed to be a real-valued variable that follows Gaussian distribution within its restricted range $[0, 1]$. Thus, the mapping function between the latent and the observed variable is defined as the following [27]:

$$y'_* = f_*, \text{ if } 0 \le f_* \le 1. \tag{3}$$

In other words, y'_* is modeled to follow a two-sided truncated Gaussian distribution. The probability density function of y'_* given the distribution of f_* can be written as the following:

$$\begin{aligned} y'_* | \mu_{\overline{f}_*}, \sigma_{\overline{f}_*} &\sim TN(\mu_{\overline{f}_*}, \sigma_{\overline{f}_*}, a = 0, b = 1) \\ &= \begin{cases} \dfrac{\frac{1}{\sigma_{\overline{f}_*}} \phi\left(\frac{y'_* - \mu_{\overline{\mathbf{f}}_*}}{\sigma_{\overline{f}_*}} \right)}{\Phi\left(\frac{1 - \mu_{\overline{f}_*}}{\sigma_{\overline{f}_*}} \right) - \Phi\left(\frac{-\mu_{\overline{f}_*}}{\sigma_{\overline{f}_*}} \right)}, & \text{if } 0 \le y'_* \le 1 \\ 0, & \text{otherwise} \end{cases} \end{aligned} \tag{4}$$

where TN represents the truncated Gaussian (Normal) distribution, and $\phi(\cdot)$ and $\Phi(\cdot)$ represent the probability density function and the cumulative distribution function of the standard Gaussian distribution, respectively.

The first step of the mapping procedure (i.e., the inference step that evaluates f_*) can be formulated as

$$p(f_* | \boldsymbol{X}, \boldsymbol{y'}, \boldsymbol{x}_*) = \int p(f_* | \boldsymbol{X}, \boldsymbol{x}_*, \boldsymbol{f}) p(\boldsymbol{f} | \boldsymbol{X}, \boldsymbol{y'}) d\boldsymbol{f} \tag{5}$$

where $p(f_* | \boldsymbol{X}, \boldsymbol{x}_*, \boldsymbol{f})$ is the equation for predicting the latent variable as in (2) assuming noiseless observation (i.e., $\boldsymbol{f} = \mathbf{y}$), and $p(\boldsymbol{f} | \boldsymbol{X}, \mathbf{y}')$ represents the posterior probability of the latent variable $\boldsymbol{f}$ given the training data. The relationship between $\boldsymbol{f}$ and $\mathbf{y}'$ can be defined as $\boldsymbol{f} = \mathbf{y}'$ based on the definition of the mapping function in (3) and the fact that the observed training data $\mathbf{y}'$ is already in the range $[0, 1]$. In other words, the mapping from $\mathbf{y}'$ to $\boldsymbol{f}$ is deterministic, and thus, $\boldsymbol{f}$ is independent of $\boldsymbol{X}$ given $\mathbf{y}'$. Then, the posterior probability can be defined as

$$\begin{aligned} p(\boldsymbol{f} | \boldsymbol{X}, \mathbf{y}') &= p(\boldsymbol{f} | \mathbf{y}') \\ &= \delta(\boldsymbol{f} - \mathbf{y}') \end{aligned}$$

where $\delta(\cdot)$ is a Dirac delta function. Substituting the aforementioned equation into (5) yields

$$\begin{aligned} p(f_* | \boldsymbol{X}, \boldsymbol{y'}, \boldsymbol{x}_*) &= \int p(f_* | \boldsymbol{X}, \boldsymbol{x}_*, \boldsymbol{f}) \delta(\boldsymbol{f} - \boldsymbol{y'}) d\boldsymbol{f} \\ &= p(f_* | \boldsymbol{X}, \boldsymbol{x}_*, \boldsymbol{f})|_{\boldsymbol{f} = \boldsymbol{y'}} \end{aligned}$$

which summarizes that the inference of the latent variable is identical to the conventional GPR procedure by substituting the observed values $\boldsymbol{y'}$ into $\boldsymbol{f}$.

The second step of the mapping procedure, i.e., the mapping from f_* to y'_*, is already defined in (3). The mean and the variance of each output y'_* can be, respectively, computed as

$$\begin{aligned}\mu_{\overline{y'}_*} &= E(y'_*|\mu_{\overline{f}_*}, \sigma_{\overline{f}_*}) \\ &= \mu_{\overline{f}_*} + \frac{\phi\left(\frac{-\mu_{\overline{f}_*}}{\sigma_{\overline{f}_*}}\right) - \phi\left(\frac{1-\mu_{\overline{f}_*}}{\sigma_{\overline{f}_*}}\right)}{\Phi\left(\frac{1-\mu_{\overline{f}_*}}{\sigma_{\overline{f}_*}}\right) - \Phi\left(\frac{-\mu_{\overline{f}_*}}{\sigma_{\overline{f}_*}}\right)} \cdot \sigma_{\overline{f}_*}, \text{ and} \\ \sigma^2_{\overline{y'}_*} &= \sigma^2_{\overline{f}_*}\left[1 + \frac{\frac{-\mu_{\overline{f}_*}}{\sigma_{\overline{f}_*}} \cdot \phi\left(\frac{-\mu_{\overline{f}_*}}{\sigma_{\overline{f}_*}}\right) - \frac{1-\mu_{\overline{f}_*}}{\sigma_{\overline{f}_*}} \cdot \phi\left(\frac{1-\mu_{\overline{f}_*}}{\sigma_{\overline{f}_*}}\right)}{\Phi\left(\frac{1-\mu_{\overline{f}_*}}{\sigma_{\overline{f}_*}}\right) - \Phi\left(\frac{-\mu_{\overline{f}_*}}{\sigma_{\overline{f}_*}}\right)}\right. \\ &\qquad \left. - \left(\frac{\phi\left(\frac{\mu_{\overline{f}_*}}{\sigma_{\overline{f}_*}}\right) - \phi\left(\frac{1-\mu_{\overline{f}_*}}{\sigma_{\overline{f}_*}}\right)}{\Phi\left(\frac{1-\mu_{\overline{f}_*}}{\sigma_{\overline{f}_*}}\right) - \Phi\left(\frac{-\mu_{\overline{f}_*}}{\sigma_{\overline{f}_*}}\right)}\right)^2\right].\end{aligned} \tag{6}$$

The addition of noise variance to the latent variable will simply replace $\mu_{\overline{f}_*}$ and $\sigma^2_{\overline{f}_*}$ with $\mu_{\overline{f}_*} = \mu_{\overline{f}_*}$ and $\sigma^2_{\overline{y}_*} = \sigma^2_{\overline{f}_*} + \sigma^2_n$, respectively.

E. Feature Selection

A wrapper-based feature selection algorithm is employed to reduce redundancies in the training set of independent variables. It evaluates feature subsets in the predefined feature searching space, and selected a feature subset that produces the best regression performance [28]. This study defines the feature searching space based on exhaustive searching, which considers all possible combinations of feature subsets. Each feature set in the searching space is evaluated as the following. The training dataset $\{\boldsymbol{X}, \boldsymbol{y}\}$ is further divided into a learning set $\{\boldsymbol{X}_l, \boldsymbol{y}_l\}$ and a validation set $\{\boldsymbol{x}_v, y_v\}$ using a leave-one-out cross validation (LOOCV). During each iteration of the LOOCV, the learning set is trained using the GPR and a prediction is made on the validation variable $\boldsymbol{x}_v$. Then, the mean standardized log loss (MSLL) [25] is used to evaluate each feature subset

$$\eta = -\frac{1}{n}\sum_{j=1}^{n} \log p(y_{v,j}|\boldsymbol{X}_{l,j}, \boldsymbol{y}_{l,j}, \boldsymbol{x}_{v,j}) \tag{7}$$

where $p(y_{v,j}|\boldsymbol{X}_{l,j}, \boldsymbol{y}_{l,j}, \boldsymbol{x}_{v,j})$ represents the predictive probability of the validation label at each LOOCV iteration j, which can be computed using (4). The feature subset that produces the minimum MSLL is selected.

V. Experimental Setup

This paper predicts postoperative physiological condition of patients using two different measures: postoperative ODI and MAA scores. A more comprehensive MAA is considered by averaging the sinusoidal MAA and step MAA, i.e., $\boldsymbol{y} = \frac{1}{2}(\alpha' + \beta')$, rather than predicting MAAs for sinusoidal and step tracks separately. Preliminary investigation of postoperative MAA scores showed that these two tracks share redundant information; the coefficient of determination was equal to 0.766 with $p < 1.69 \times 10^{-7}$.

The prediction performance of GPR is evaluated using an LOOCV. The entire data are divided into a training dataset $D_i = \{\boldsymbol{X}_i, \boldsymbol{y}_i\}$ and a testing dataset $\boldsymbol{x}_{*,i}$ at each iteration i of LOOCV. At each iteration, the feature selection algorithm is performed on the training data, which eventually performs another (inner) layer of an LOOCV to select the best feature subset as discussed in Section IV-E. The GPR is trained on the dimension-reduced training data, and a prediction is made on $\boldsymbol{x}_{*,i}$ to produce $\mu_{\overline{y'}_{*,i}}$ and $\sigma_{\overline{y'}_{*,i}}$ based on (6). This approach, which completely isolates the testing set from selection of features and parameters, provides a fair estimate of prediction performance rather than an optimistic estimate [29]. The same evaluation procedure has been applied to the three benchmarking models considered for comparison: multivariate linear regressions (MLR), support vector regression (SVR), and *K*-nearest neighbors regression (KNN).

VI. Experimental Results

A. Prediction of Postoperative ODI

The prediction results are summarized in Fig. 2. The *x*-axis of Fig. 2(a) represents the actual ODI that the patient evaluated after the surgery and the *y*-axis represents the predicted mean ODI ($\mu_{\overline{y'}_*}$) with confidence range of one standard deviation ($\sigma_{\overline{y'}_*}$) based on (6). Note that the prediction variable follows a truncated Gaussian distribution, and thus, the variance (or standard deviation) does not provide any information regarding the percentile of the predicted values; it simply measures the amount of dispersion from the predicted mean. Fig. 2(b) depicts the Bland–Altman plot of the predicted mean and the ground truth. The bias and the limit of agreements were, respectively, computed as -0.025 and 0.196, which showed that the two methods were systematically producing similar results. Furthermore, there was no trend along the *x*-axis and the variability of the difference was consistent. This emphasizes that the prediction model produced consistent predictions for different ranges.

The numerical evaluation of the prediction is summarized in Table II using the coefficient of determination (R^2), the mean absolute difference (MAD) between the predicted mean and the ground truth, the p-value, and the MSLL as in (7). Table II compares the results of the proposed truncated GPR, which considers the restricted range of the dependent variables as in (6), against the conventional GPR as in (2). Truncated GPR provided superior prediction performance with MAD of 0.079 (out of maximum MAD of 1.00) compared to the conventional GPR with MAD of 0.112. The prediction performances of the proposed method were also compared to the three benchmarking prediction models: MLR, KNN regression, and SVR with the radial basis function kernel. MLR assumes oversimplified linear relationships between the independent and the dependent variables, and as a consequence, it achieved the worst MAD of 0.148. SVR is a nonparametric model similar to GPR. Especially, the radial basis function kernel SVR is considered identical to GPR since the kernel function can be defined exactly as (2). Although the examined SVR employed a simplified

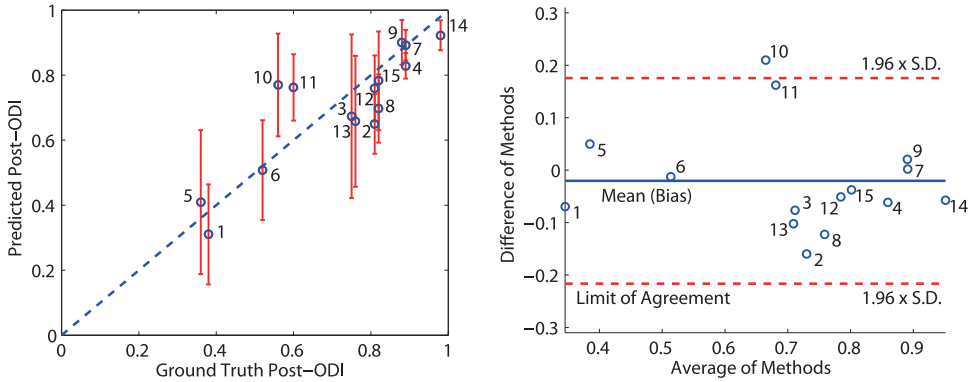

(a) (b)

Fig. 2. Prediction of postoperative ODI using the proposed truncated GPR. (a) Scatter of predicted mean with one standard deviation, which achieved MAD of 0.079, R^2 of 0.716, MSLL of 3.83, and $p < 4.7 \times 10^{-5}$. (b) Bland–Altman plot of the predicted mean with the bias of -0.025 and the limit of agreement of 0.196.

TABLE II
SUMMARY OF THE NUMERICAL EVALUATION OF VARIOUS TECHNIQUES USED IN THIS STUDY FOR PREDICTING ODI (LEFT) AND MAA (RIGHT) SCORES

Prediction	ODI				MAA			
Method	MAD	R^2	MSLL	p-value	MAD	R^2	MSLL	p-value
Truncated GPR	0.079	0.668	3.83	4.7×10^{-5}	0.014	0.591	1.87	2.8×10^{-4}
Conventional GPR	0.112	0.443	3.96	3.5×10^{-3}	0.015	0.588	1.86	3.3×10^{-4}
MLR	0.148	0.081	N/A	0.136	0.027	0	N/A	0.148
SVR	0.117	0.448	N/A	5.0×10^{-3}	0.019	0.497	N/A	6.3×10^{-4}
KNN	0.121	0.437	N/A	5.8×10^{-3}	0.024	0.067	N/A	0.017

Note that N/A stands for "not available."

TABLE III
SUMMARY OF THE FEATURE SETS SELECTED DURING THE LOOCV FOR PREDICTING ODI AND MAA

Predicting ODI		Predicting MAA	
Selected Features	Freq.	Selected Features	Freq.
ρ, α	10	ρ, α, g	11
ρ, α, r	3	ρ, α, β, r	1
ρ, α, β	1	ρ, α, g, r	1
ρ, α, h	1	ρ, β, r	1
		ρ, r	1

Freq. represents the frequency of the selected feature set.

TABLE IV
MEAN AND THE STANDARD DEVIATION OF HYPERPARAMETERS (AT THE MODE) DURING THE LOOCV

	Predicting ODI		Predicting MAA	
	Mean $\pm$ Std. Dev	Freq.	Mean $\pm$ Std. Dev	Freq.
ℓ_ρ	0.25 ± 0.06	15	0.40 ± 0.08	15
ℓ_α	0.01 ± 0.05	15	0.23 ± 0.01	13
ℓ_β	$0.05 \pm$ N/A	1	0.12 ± 0.08	2
ℓ_g	N/A	0	0.31 ± 0.02	12
ℓ_r	1.1 ± 0	3	4.80 ± 8.78	4
ℓ_h	$4.5 \pm$ N/A	1	N/A	0
σ_f	0.63 ± 0.03	15	0.75 ± 0.03	15
σ_n	$1.0 \cdot 10^{-4} \pm 2.9 \cdot 10^{-20}$	15	$9.8 \cdot 10^{-6} \pm 1.4 \cdot 10^{-17}$	15

kernel function (i.e., $k(\boldsymbol{x}, \boldsymbol{x'}) = \exp(-(\boldsymbol{x} - \mathbf{x}')^{\mathrm{T}} M(\boldsymbol{x} - \boldsymbol{x'}))$, where $M = \gamma \boldsymbol{I}$), SVR produced comparable prediction performance (i.e., MAD of 0.117) to the conventional GPR. KNN regression is another nonparametric method, which also produced comparable MAD of 0.121. These three methods only provide single-valued predictions rather than probabilistic predictions and assume that the dependent variables follow Gaussian distributions. It implies that these methods cannot be configured to the restricted value range of the predictor variables, and thus, lead to inferior prediction performances compared to the proposed truncated GPR. Note that MSLL is not available for these three regression models as they do not make probabilistic predictions.

A one-way analysis of variance was performed on the preoperative and the postoperative ODI values, and produced $p < 0.188$ with MAD of 0.145, which supports the necessity of a prediction model. This can be considered as a result of an elementary prediction model that assumes no difference in ODI values. It is noteworthy that MLR produced results that are inferior compared to this simple model, which seems to be caused by the heavily nonlinear relationships between predictors (other than the preoperative ODI) and the postoperative ODI.

As discussed in Section V, GPR predictions were made in an LOOCV manner and as a result, n different prediction models (i.e., selected features and the values of hyperparameters) were created. The selected features and the values of hyperparameters at the mode (i.e., most likely hyperparamters) are summarized in Tables III and IV, respectively. Table III shows that $\{\rho, \alpha\}$ is the most frequently selected feature set and is also a subset of all

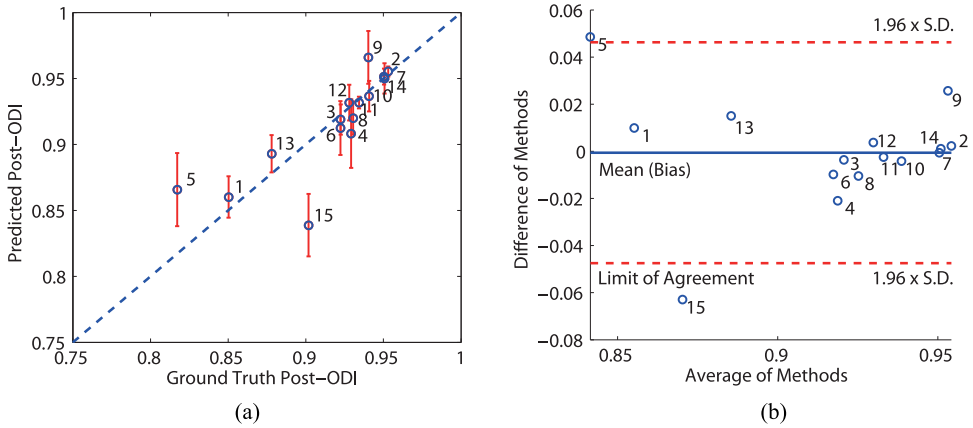

Fig. 3. Prediction of postoperative MAA using the proposed truncated GPR. (a) Scatter of predicted mean with one standard deviation, which achieved MAD of 0.014, R^2 of 0.591, MSLL of 1.87, and $p < 2.8 \times 10^{-4}$. (b) Bland–Altman plot of the predicted mean with the bias of -6.0×10^{-4} and the limit of agreement of 0.047.

other selected feature sets. This demonstrates that there exists a consistent pattern within the constructed regression models. Table IV shows that $\ell_\rho, \ell_\alpha, \sigma_f$, and σ_n were the hyperparameters that were used more than 12 times (i.e., 80%) to construct prediction models during an LOOCV. Small variances of the selected parameter values support that the selected values were consistent. Furthermore, $\ell_\rho = 0.25$ and $\ell_\alpha = 0.10$ characterize relatively flexible (nonlinear) covariance function rather than simple linear relationship. As a consequence, the noise parameter is reduced to $\sigma_n = 1.0 \times 10^{-4}$.

In order to quantify the contributions of the target tracking results in predicting ODI, the prediction procedure was performed with α and β being removed from the feature set. This allows the comparison between a feature set that contains the target tracking results (see Table II) and a feature set constructed solely based on demographic and clinical variables. The prediction results without hand motor scores achieved an MAD of 0.118, a R^2 of 0.297, an MSLL of 3.89, and a $p < 0.0166$. These results show that incorporating the handgrip test for predicting postoperative functional outcomes significantly improves the accuracy (i.e., MAD by 0.039).

B. Prediction of Postoperative MAA

A similar procedure has been taken for predicting postoperative MAA. The results are illustrated in Fig. 3(a) and (b), which show that data points #5 and #15 produced the largest errors in the mean prediction. Patient #5 was the patient whose hand motor score decreased with the largest drop, and patient #15 was the patient whose hand motor score increased with the largest gain. As a consequence, the prediction model have, respectively, overpredicted and underpredicted the MAA scores for these patients. This result may be due to the relatively small size of the examined data, which does not effectively construct models for these possibly outlying patients. Nonetheless, the prediction results of postoperative MAA were much more accurate compared to ODI as summarized in Table II. Furthermore, the bias and the limit of agreement of the Bland–Altman plot in Fig. 3(b) were -6.0×10^{-4} and 0.047, respectively, which support higher consistency compared to ODI prediction.

The proposed truncated GPR model produced the most superior results (MAD of 0.014 with $p < 2.8 \times 10^{-4}$) compared to other benchmarking models (see Table II). However, the differences in MAD and MSLL values compared to the conventional GPR were negligible due to extremely small $\sigma^2_{f_*}$. Consequently, the truncated GPR, the conventional GPR, and SVR produced comparable prediction performances.

MLR and KNN regression produced MAD of 0.027 and 0.024, respectively. Considering that the elementary prediction model, which assumes no difference in MAA after the surgery, produced MAD of 0.024 with $p < 0.128$, both MLR and KNN regression model did not much improve the prediction accuracy. In particular, MLR produced results that are worse than this simple mapping function, which again support the needs for a nonlinear kernel in predicting postoperative conditions of these patients.

The selected features are summarized in Table III, which shows that $\{\rho, \alpha, g\}$ is the most frequently selected feature subset. Furthermore, Table IV also shows that $\ell_\rho, \ell_\alpha, \ell_g, \sigma_f$, and σ_n are the features that were selected at least 12 times (i.e., 80%) during the LOOCV iterations. Similarly to the ODI results, the values of hyperparameters characterize relatively flexible covariance function with small noise variance $\sigma_n = 9.8 \times 10^{-6}$.

VII. Discussion and Conclusion

This paper introduces a prediction method for postoperative functional outcomes by a novel use of GPR. Two functional outcomes are considered in this paper: ODI and the target tracking score. The proposed method has been compared against three widely used benchmarking prediction models (i.e., MLR, SVR, and KNN regression), and showed superior prediction performance.

By predicting the postoperative outcomes using preoperative data, it is assumed that the surgical operation performed on the patient produces a constant success pattern. The patients in this study have received the surgical operation from a single neurosurgeon, and thus, this assumption is valid to an extent. The constructed model fundamentally incorporates this pattern of surgical results, which may vary depending on the

preoperative condition of the patient. Consequently, the model reported in this paper may not produce the same result on patients performed by other surgeons (especially when the data size is small) as the surgical skill can be varied. However, the proposed method can be easily applied to individual surgeons, and moreover, the problem of variation in surgical skills among different surgeons can be resolved as a large-scale dataset is incorporated to generalize the pattern.

This study enables new opportunities for accurate prediction of postoperative conditions of individuals with neuromuscular deficits using GPR. It further enables clinicians to perform more ubiquitous and convenient screening (using the handgrip device) for predicting a patient's functional level before the medical treatment, which can be especially beneficial to the patients, their care givers, and physical therapists.

REFERENCES

[1] H. Al-Nashash, N. Fatoo, N. Mirza, R. Ahmed, G. Agrawal, N. Thakor, and A. All, "Spinal cord injury detection and monitoring using spectral coherence," *IEEE Trans. Biomed. Eng.*, vol. 56, no. 8, pp. 1971–1979, Aug. 2009.

[2] L. Sekhon and M. G. Fehlings, "Epidemiology, demographics, and pathophysiology of acute spinal cord injury," *Spine*, vol. 26, no. 24S, pp. S2–S12, 2001.

[3] H. K. Lim, D. C. Lee, W. B. McKay, M. M. Priebe, S. A. Homes, and A. M. Sherwood, "Neurophysiological assessment of lower-limb voluntary control in incomplete spinal cord injury," *Spinal Cord.*, vol. 43, pp. 283–290, 2005.

[4] J. A. Tracy and J. D. Bartleson, "Cervical spondylotic myelopathy," *The Neurologist*, vol. 16, pp. 176–187, 2010.

[5] M. H. Lipper, J. H. Goldstein, and H. M. Do, "Brown-sequard syndrome of the cervical spinal cord after chiropractic manipulation," *Amer. J. Neuroradiol.*, vol. 17, pp. 1349–1352, 1998.

[6] J. A. Kopec, "Measuring functional outcomes in persons with back pain: A review of back-specific questionnaires," *Spine*, vol. 15, pp. 3110–3114, 2000.

[7] C. Bombardier, "Outcome assessments in the evaluation of treatment of spinal disorders: Summary and general recommendations," *Spine*, vol. 25, no. 24, pp. 3100–3103, 2000.

[8] J. A. Finkelstein, "Response shift following surgery of the lumbar spine," Master's thesis, University of Toronto, Toronto, ON, Canada, 2010.

[9] E. M. Adang, G. Kootstra, G. L. Engel, J. P. van Hooff, and H. L. Merckelbach, "Do retrospective and prospective quality of life assessments differ for pancreas-kidney transplant recipients?" *Transplant Int.*, vol. 11, pp. 11–15, 1998.

[10] M. W. Post, L. P. de Witte, F. W. van Asbeck, A. J. van Dijk, and A. J. Schrijvers, "Predictors of health status and life satisfaction in spinal cord injury," *Arch. Phys. Med. Rehabil.*, vol. 79, no. 4, pp. 395–401, 1998.

[11] M. P. Dijkers, "Correlates of life satisfaction among persons with spinal cord injury," *Arch. Phys. Med. Rehabil.*, vol. 80, no. 8, pp. 867–876, 1999.

[12] M. Tonack, S. L. Hitzig, B. C. Craven, K. A. Campbell, K. A. Boschen, and C. F. McGillivray, "Predicting life satisfaction after spinal cord injury in a canadian sample," *Spinal Cord*, vol. 46, pp. 380–385, 2008.

[13] S. D. Pradhan, B. R. Brewer, G. E. Carvell, P. J. Sparto, A. Delitto, and Y. Matsuoka, "Assessment of fine motor control in individuals with Parkinson's disease using force tracking with a secondary cognitive task," *J. Neurol. Phys. Therapy*, vol. 34, no. 1, pp. 32–40, 2010.

[14] S. K. Naik, C. Patten, N. Lodha, S. A. Coombes, and J. H. Cauraugh, "Force control deficits in chronic stroke: grip formation and release phases," *Exp. Brain Res.*, vol. 211, no. 1, pp. 1–15, 2011.

[15] S. Lee, H. Ghasemzadeh, B. Mortazavi, and M. Sarrafzadeh, "A pervasive assessment of motor function: A lightweight grip strength tracking system," *IEEE J. Biomed. Health Informat.*, vol. 17, no. 6, pp. 1023–1030, Nov. 2013.

[16] R. Getachew, S. Lee, J. Kimball, A. Yew, D. Lu, C. Li, J. Garst, N. Ghalehsari, B. Paak, M. Razaghy, M. Espinal, A. Ostowari, A. Ghavamrezaii, S. Pourtaheri, I. Wu, M. Sarrafzadeh, and D. Lu, "Utilization of a novel digital measurement tool for quantitative assessment of upper extremity motor dexterity: A controlled pilot study," *J. NeuroEng. Rehabil.*, vol. 11, no. 1, pp. 1–9, 2014.

[17] J. M. Veerbeek, G. Kwakkel, E. E. van Wegen, J. C. Ket, and M. W. Heymans, "Early prediction of outcome of activities of daily living after stroke: A systematic review," *Stroke*, vol. 42, no. 5, pp. 1482–1488, 2011.

[18] S.-E. Soh, M. E. Morris, and J. L. McGinley, "Determinants of health-related quality of life in parkinsons disease: A systematic review," *Parkinsonism Related Disorders*, vol. 17, no. 1, pp. 1–9, 2011.

[19] O. Stegle, S. Fallert, D. J. C. MacKay, and S. Brage, "Gaussian process robust regression for noisy heart rate data," *IEEE Trans. Biomed. Eng.*, vol. 55, no. 9, pp. 2143–2151, Sep. 2008.

[20] T. M. Hope, M. L. Seghier, A. P. Leff, and C. J. Price, "Predicting outcome and recovery after stroke with lesions extracted from MRI images," *NeuroImage: Clinical*, vol. 2, pp. 424–433, 2013.

[21] J. Fairbank and P. B. Pynsent, "The oswestry disability index," *Spine*, vol. 25, no. 22, pp. 2940–2953, 2000.

[22] L. T. Holly, P. G. Matz, P. A. Anderson, M. W. Groff, R. F. Heary, M. G. Kaiser, P. V. Mummaneni, T. C. Ryken, T. F. Choudhri, E. J. Vresilovic, and D. K. Resnick, "Clinical prognostic indicators of surgical outcome in cervical spondylotic myelopathy," *J. Neurosurg.: Spine*, vol. 11, no. 2, pp. 112–118, 2009.

[23] R. Jones, *Measurement of Sensory-Motor Control Performance Capacities: Tracking Tasks*. Boca Raton, FL, USA: CRC Press, 2000.

[24] G. Kondraske, *A Working Model for Human System-Task Interfaces*. Boca Raton, FL, USA: CRC Press, 1995.

[25] C. E. Rasmussen and C. K. I. Williams, *Gaussian Processes for Machine Learning*. Cambridge, MA, USA: MIT Press, 2006.

[26] V. Pietilainen, "Approximations for integration over the hyperparameters in Gaussian processes," Master's thesis, Aalto University, Espoo, Finland, 2010.

[27] W. H. Greene, *Censored Data and Truncated Distributions in Palgrave Handbook of Economics*. New York, NY, USA: Palgrave Macmillan, 2006.

[28] I. Guyon and A. Elisseeff, "An introduction to variable and feature selection," *J. Mach. Learn. Res.*, vol. 3, pp. 1157–1182, Mar. 2003.

[29] L. Palmerini, S. Mellone, G. Avanzolini, F. Valzania, and L. Chiari, "Quantification of motor impairment in Parkinson's disease using an instrumented timed up and go test," *IEEE Trans. Neural Syst. Rehabil. Eng.*, vol. 21, no. 4, pp. 664–673, Jul. 2013.

Sunghoon Ivan Lee (S'12) received the Ph.D. degree in computer science from the University of California Los Angeles, Los Angeles, CA, USA, in 2014.

He is currently a Postdoctoral Research Associate in the Department of Physical Medicine & Rehabilitation, Harvard Medical School, Boston, MA, USA. His main research interests include wearable body sensors, biomedical signal processing, data analytics, and user interface design for smart and mobile health applications.

Bobak Mortazavi (S'12) received the Ph.D. degree from the University of California Los Angeles, Los Angeles, CA, USA, in 2014.

After receiving the Ph.D. degree, he joined the Yale University School of Medicine, New Haven, CT, USA, as a Postdoctoral Associate in 2014. His research interests include wearable sensors, embedded systems, and machine learning applications for wireless health research, developing systems and predictions for personalized health applications.

Eunjeong Park (M'07) received the Ph.D. degree in computer science and engineering from the Seoul National University, Seoul, Korea, in 2006.

She is currently a Research Manager with Wireless Health Institute, University of California, Los Angeles, CA, USA and a Research Professor at the Embedded System Research Center, Ewha WomansUniversity, Seoul. Her current research interests include healthcare systems, intelligent medical informatics, and mobile computing.

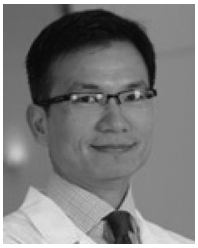

Daniel C. Lu is currently an Associate Professor of neurosurgery and orthopedic surgery at the University of California Los Angeles (UCLA), Los Angeles, CA, USA. As the Principal Investigator of the Neuroplasticity and Repair Laboratory and the Director of UCLA Neuromotor Recovery and Rehabilitation Center, his research interests include modulating the neuronal circuitry and networks of the spinal cord in the treatment of neuromotor disorders. His research is funded by the National Institutes of Health and Department of Defense. His clinical expertise involves minimally invasive techniques in the surgical management of degenerative, traumatic, neoplastic, and spinal disorders.

Majid Sarrafzadeh (M'82–SM'92–F'96) received the Ph.D. degree in electrical and computer engineering from the University of Illinois at Urbana-Champaign, Champaign, IL, USA, in 1987.

From 1987 to 2000, he served as a Professor in the Electrical and Computer Engineering Department, Northwestern University, Evanston, IL, USA. In 2000, he joined the faculty at Computer Science Department, University of California Los Angeles (UCLA), Los Angeles, CA, USA, where in 2014, he became a Distinguished Professor of computer science. He serves as the Codirector for the UCLA Wireless Health Institute and the BRITE center on Minority Health Disparities. His research interests include wireless health research, embedded systems, and the design and implementation of novel analytic algorithms for wireless health applications.

Haydn Hoffman, Derek Lu, Charles Li, Brian Paak, Jordan Garst, Mehrdad Razaghy, and Marie Espinal photographs and biographies not available at the time of publication .